Extraction of Red Edge Optical Parameters From Hyperion Data for Estimation of Forest Leaf Area Index

Ruiliang Pu, Peng Gong, Greg S. Biging, and Mirta Rosa Larrieu

***Abstract*—A correlation analysis was conducted between forest leaf area index (LAI) and two red edge parameters: red edge position (REP) and red well position (RWP), extracted from reflectance image retrieved from Hyperion data. Field spectrometer data and LAI measurements were collected within two days after the Earth Observing One satellite passed over the study site in the Patagonia region of Argentina. The two red edge parameters were extracted with four approaches: four-point interpolation, polynomial fitting, Lagrangian technique, and inverted-Gaussian (IG) modeling. Experimental results indicate that the four-point approach is the most practical and suitable method for extracting the two red edge parameters from Hyperion data because only four bands and a simple interpolation computation are needed. The polynomial fitting approach is a direct method and has its practical value if hyperspectral data are available. However, it requires more computation time. The Lagrangian method is applicable only if the first derivative spectra are available; thus, it is not suitable to multispectral remote sensing. The IG approach needs further testing and refinement for Hyperion data.**

***Index Terms*—Hyperion, leaf area index, red edge position, red well position.**

I. Introduction

LEAF AREA INDEX (LAI) is an important structural parameter for quantifying the energy and mass exchange characteristics of terrestrial ecosystems, such as photosynthesis, respiration, transpiration, carbon and nutrient cycle, and rainfall interception (e.g., see [1]–[4]). Direct measurement of canopy LAI is labor intensive and time consuming. Remote sensing techniques, particularly satellite remote sensing, may offer a practical means of LAI measurement at the landscape and global scales [5]. With remote sensing, a number of forest ecosystem variables can be estimated, including LAI, absorbed fraction of photosynthetically active radiation (fAPAR), canopy temperature, and community type. Ratio indices between near-infrared (NIR) and red reflectance were positively related to forest LAI across a variety of environments (e.g., see [3] and [5]–[7]). However, a weak relation between vegetation indexes (VIs) and forest LAI has been shown when 1) canopy cover is low and 2) there is spatial variation in understory reflectance (e.g., see [8] and [9]). This is attributed to sensitivity of VIs to changes of plant reflectance and transmittance characteristics, caused by various environmental factors [10], [11]. Red edge parameters, compared to VIs, are relatively insensitive to changes of biophysical factors, such as soil cover percentage and optical properties [10], [12], [13], canopy structure and leaf optical properties [10], [14], atmospheric effects [15], and irradiance and solar zenith angle [10], [14]. Hyperspectral data can be used to extract red edge optical parameters, which are useful for estimating such biophysical and biochemical parameters as LAI, chlorophyll content (e.g., see [16] and [17]) and vegetation stress. Airborne and spaceborne imaging spectrometers now have the potential for determining the red edge parameters of vegetation canopies at the regional scale [18].

There are two primary red edge optical parameters—red edge position (REP) and red well position (RWP). REP, located between 680 and 750 nm, is defined as the wavelength of the inflection point of the reflectance slope at the red edge. Experimental and theoretical studies show that it shifts according to changes of chlorophyll content [17], [19], LAI [16], biomass and hydric status [20], age [21], plant health levels [22], and seasonal patterns [23]. When a plant is healthy with high chlorophyll content and high LAI, the red edge position shifts toward the longer wavelengths; when it suffers from disease or chlorosis and low LAI, it shifts toward the shorter wavelengths. Researchers have demonstrated this behavior of the red edge using spectral reflectance measurements obtained either in the laboratory or from airborne sensors. RWP is the wavelength position corresponding to a plant's minimum reflectance in red (maximum chlorophyll absorption), which also functions as REP [17].

Currently, there are four major spectra used for extraction of red edge optical parameters: modeling spectra (e.g., [10]), laboratory-measured spectra (e.g., [23]), *in situ* field spectra (e.g., [20]), and airborne imaging spectra (e.g., [13]). In this study, new hyperspectral data (Hyperion data) were first used to extract the two red edge optical parameters with four existing methods (see Section III). Hyperion is the first satellite hyperspectral sensor [24]. Therefore, the objectives of this study were to test and compare the performance of all four existing approaches for extracting the two red edge parameters from Hyperion data for forest LAI estimation.

Manuscript received October 28, 2002; revised March 18, 2003. This research was supported in part by the National Aeronautics and Space Administration under EO-1 Science Validation Grant NCC5-492. Field support was provided by the Forest Plantation Inventory Section of the Secretariat of Agriculture, Livestock, Fisheries and Food of the government of Argentina.

R. Pu, P. Gong, and G. S. Biging are with the Center for Assessment and Monitoring of Forest and Environmental Resources (CAMFER), University of California, Berkeley, CA 94720-3110 USA (e-mail: rpu@nature.berkeley.edu).

M. R. Larrieu is with the Proyecto Forestal de Desarrollo, Secretaría de Agricultura, Ganaderìa, Pesca y Alimentación, 1063 Buenos Aires, Argentina.

Digital Object Identifier 10.1109/TGRS.2003.813555

II. Study Site and Datasets

During the 2001 Earth Observing One campaign in Argentina, we established a study site (41° 10′ 59″ S/71° 20′ 27″ W) in Rio Negro province in the Patagonia region of southern Argentina. The study area is a relatively flat semiarid region with conifer forest plantations of young- to mid-aged ponderosa pine (*Pinus ponderosa*), lodgepole pine (*Pinus contorta*), and Oregon pine (*Pinus oregon*). Other broad-leaf species, shrubs, and grasses are also found at this site. The average elevation is 850 m, with variations within 100 m.

Hyperion data were acquired on March 27, 2001, around 10:30 A.M. local time. The Hyperion has 220 bands, covering 0.4–2.5 μm at approximately a 10-nm spectral resolution and a 30-m ground resolution. From March 27–28, 2001, we took reflectance measurements in the field from targets such as road surfaces (gravel material), bare soil, and young tree canopies (ponderosa pine and lodgepole pine) using a FieldSpec Pro FR (Analytical Spectral Devices, Inc.) that covers the same spectral range as Hyperion. All spectra were measured at the nadir direction of the radiometer with a 25° field of view. The distance between the spectroradiometer and the leaf samples was about 0.5–1.0 m to allow a within-target area radiance measurement. White reference current was measured every 5–10 min. Each sample was repeatedly measured ten times with the spectrometer. These spectral reflectance measurements were then used for atmospheric correction of the Hyperion data.

An LAI-2000 Plant Canopy Analyzer (PCA) was used in the field to measure forest LAI. The LAI measurement taken by the PCA is the "effective" LAI [1], [4]. From March 27–28, 2001, a total of 32 LAI measurements were taken. Each LAI measurement represents an average of ten PCA readings, which were taken in an area between 100–1000 m^2. Since the effective LAI is easier to measure than LAI, as an intrinsic attribute of plant canopies [1], we directly used the effective LAI throughout this research and referred it to as LAI.

III. Methods

A. Atmospheric Correction

In this study, we used a hybrid method [25], [26] of atmospheric correction to retrieve surface reflectance from Hyperion data because it had worked well for satellite and airborne data in our previous work. The procedure of the hybrid method can be described as follows. With MODTRAN4 modeling, at-sensor total radiances can be simulated when inputting appropriate parameters. The simulated output radiances are then used to solve a radiative transfer model for three major parameters: sun-surface-sensor two-way transmittance T_2, the path radiance caused by atmospheric scattering L_a, and the spherical albedo of the atmosphere S. Using sensor pixel radiance values as at-sensor radiance and solving T_2, S, and L_a, we can easily calculate a pixel-based surface reflectance from the Hyperion image, referred to as initial reflectance. A set of ratios across all spectral bands is calculated by dividing the ground reflectance by its corresponding initial reflectance. In order to make the ratios represent the range of available targets, an average ratio was calculated from the different targets (e.g., road surface and vegetation in this study). Multiplying the initial reflectance of each pixel by its corresponding ratio in each band, we can improve the initial reflectance. For a detailed description to the procedure, see [25] and [26]. Using this procedure, the Hyperion image was converted into the retrieved surface reflectance.

B. Approaches to Extracting the Two Red Edge Parameters

Accurate estimation of red edge parameters depends on sensor band positions and widths. Various techniques of analysis have been developed to minimize errors in determining the red edge parameters. In this analysis, four approaches were tested, since the red edge parameters determined by the four approaches were originally used for estimating leaf chlorophyll content (or concentration), canopy LAI, vegetation stress, etc.

1) Four-Point Interpolation: The REP is defined as the wavelength position of the greatest first-order derivative spectrum. Because the spectral resolution of the Hyperion data is relatively low (10 nm), a four-point interpolation was used [10], [16]. The linear interpolation as described in [10] assumes that the reflectance curve at the red edge can be simplified to a straight line centered near a midpoint between 670 and 780 nm. The REP interpolated in [10] locates in the range between 700 and 740 nm. There are two steps for calculating REP: 1) calculate the reflectance at the inflection point along the red edge of reflectance [ρ_i, as in (1)]; 2) calculate the wavelength of the reflectance at the inflection point [λ_i, as in (2)]

$$\rho_i = (\rho_1 + \rho_4)/2 \tag{1}$$

$$\lambda_i = \lambda_2 + (\lambda_3 - \lambda_2)\frac{\rho_i - \rho_2}{\rho_3 - \rho_2} \tag{2}$$

where $\lambda_1, \lambda_2, \lambda_3$, and λ_4 are wavelengths of 670, 700, 740, and 780 nm, respectively, and ρ_1, ρ_2, ρ_3, and ρ_4 are reflectances at corresponding wavelengths, respectively. Accordingly, another red edge parameter [RWP (λ_0)] could also be interpolated from (3)

$$\lambda_0 = \lambda_1 + (\lambda_2 - \lambda_1)\frac{\rho_i - \rho_2}{\rho_3 - \rho_2}. \tag{3}$$

Four Hyperion bands (671.62, 702.12, 742.80, and 783.48 nm) were selected in this analysis. The REP interpolated with this method was originally used for estimating leaf chlorophyll content and LAI of the plant canopy.

2) Polynomial Fitting: A red edge reflectance curve between the wavelengths corresponding to the minimum reflectance in red and the maximum NIR "shoulder" reflectance can be fitted with a fifth-order polynomial equation as

$$\rho = a_0 + \sum_{i=1}^{5} a_i \lambda^i \tag{4}$$

where λ represents 13 band wavelengths of Hyperion from 661.45–783.48 nm. The R^2 of the fifth-order polynomial model reaches values greater than 0.998 for most of the spectral samples. An advantage of this approach is that a continuous derivative curve can be generated by taking the derivative of the fifth-order polynomial curve, instead of taking differences and ratios band by band. Accordingly, we can determine the REP and RWP values for each spectral sample based on the REP and RWP definitions.

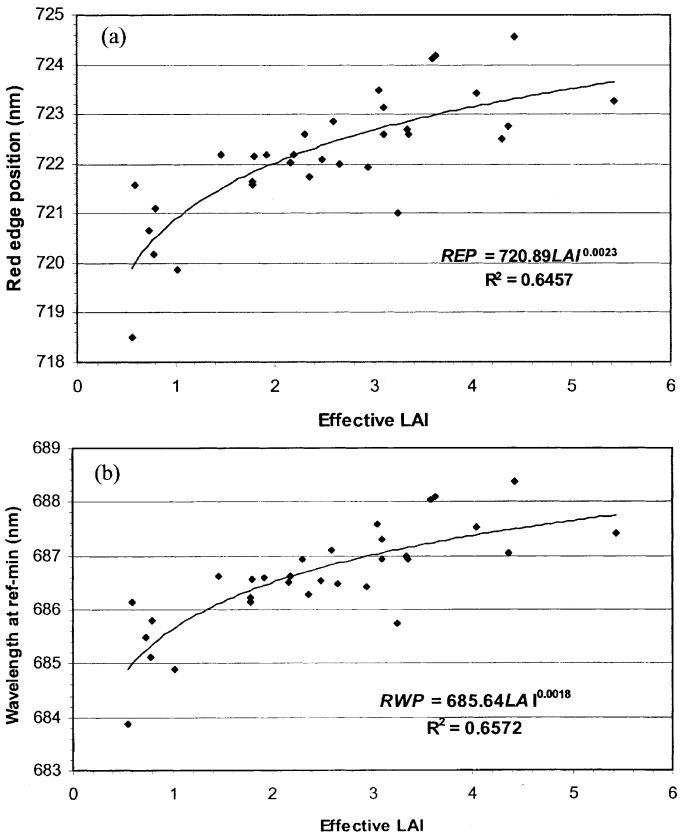

Fig. 1. Forest LAI versus two red edge parameters extracted with the four-point interpolating approach (using bands 671.62, 702.12, 742.80, and 783.48 nm). (a) LAI versus REP. (b) LAI versus RWP (minimum reflectance position).

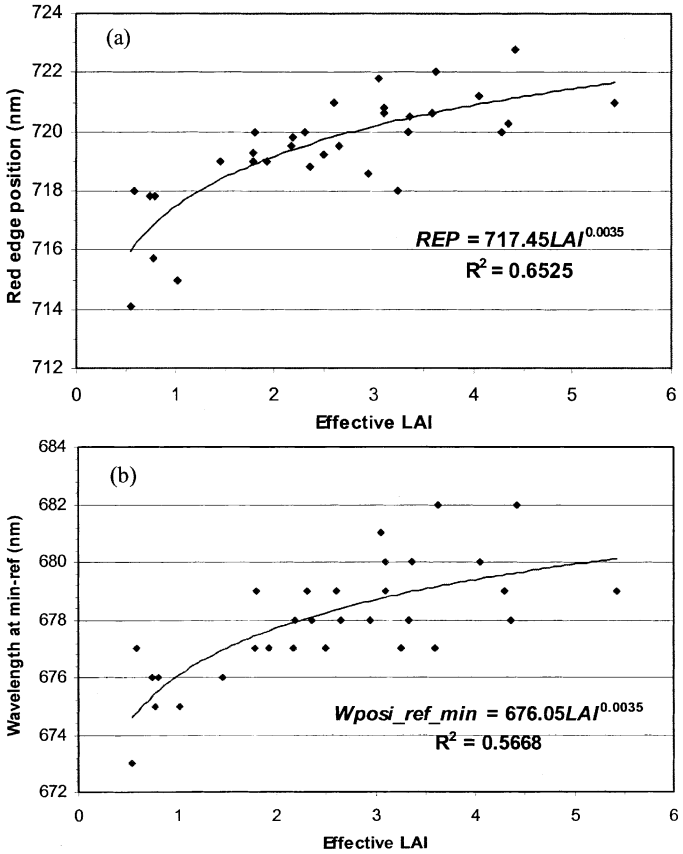

Fig. 2. Forest LAI versus two red edge parameters extracted with the polynomial fitting approach using 13 bands (wavelengths: 661.45–783.48 nm). (a) LAI versus REP. (b) LAI versus RWP (minimum reflectance position).

3) Lagrangian Technique: Dawson and Curran [18] presented a technique based upon a three-point Lagrangian interpolation for locating the REP in spectra that are sampled coarsely. They determined the REP with this interpolation technique and correlated it with leaf chlorophyll content. They concluded that this technique was very useful for observing red edge shifts. This technique is applied to the first-derivative transformation of the reflectance spectrum. The technique fits a second-order polynomial curve to the three first-derivative bands, centered near the maximum slope position. According to [18], a second derivative is then performed on the Lagrangian equation to determine the maximum slope position, i.e.,

$$\mathrm{REP} = \frac{A(\lambda_i + \lambda_{i+1}) + B(\lambda_{i-1} + \lambda_{i+1}) + C(\lambda_{i-1} + \lambda_i)}{2(A + B + C)} \tag{5}$$

where

$$A = \frac{D_{\lambda(i-1)}}{(\lambda_{i-1} - \lambda_i)(\lambda_{i-1} - \lambda_{i+1})}$$
$$B = \frac{D_{\lambda(i)}}{(\lambda_i - \lambda_{i-1})(\lambda_i - \lambda_{i+1})}$$
$$C = \frac{D_{\lambda(i+1)}}{(\lambda_{i+1} - \lambda_{i-1})(\lambda_{i+1} - \lambda_i)} \tag{6}$$

andwhere $D_{\lambda(i-1)}, D_{\lambda(i)}$, and $D_{\lambda(i+1)}$ are the first derivative values around the red edge position of the maximum slope at wavelengths λ_{i-1}, λ_i and λ_{i+1}, respectively. In this study, we used two methods to obtain the three bands of the first derivatives. One method uses the three first-derivative bands (713, 720, and 727 nm) calculated from the polynomial fitting curve (the second approach), and the other uses the three first-derivative bands (712.29, 722.46, and 732.63 nm) calculated from five neighborhood Hyperion bands from 702.12–742.80 nm.

4) Inverted-Gaussian Modeling: Based on [27], [28], the spectral shape of the red edge reflectance can be approximated by one half of an inverted-Gaussian (IG) function. Accordingly, the IG model represents the red edge as follows:

$$R(\lambda) = R_s - (R_s - R_0)\exp\left(\frac{-(\lambda_0 - \lambda)^2}{2\sigma^2}\right) \tag{7}$$

where R_s is the maximum or "shoulder" spectral reflectance; R_0 and λ_0 are the minimum spectral reflectance and corresponding wavelength (i.e., RWP), respectively; λ is wavelength; and σ^2 is the Gaussian function variance parameter. A fifth related parameter is λ_p (i.e., REP), calculated as follows:

$$\lambda_p = \lambda_0 + \sigma. \tag{8}$$

The IG model has been fitted to laboratory spectral reflectance data [28] and airborne imaging spectrometer data [29]. The red edge parameters extracted from those spectral data with the IG modeling have been used to estimate leaf chlorophyll concentration and vegetation stress [17], [27]. The IG model can be

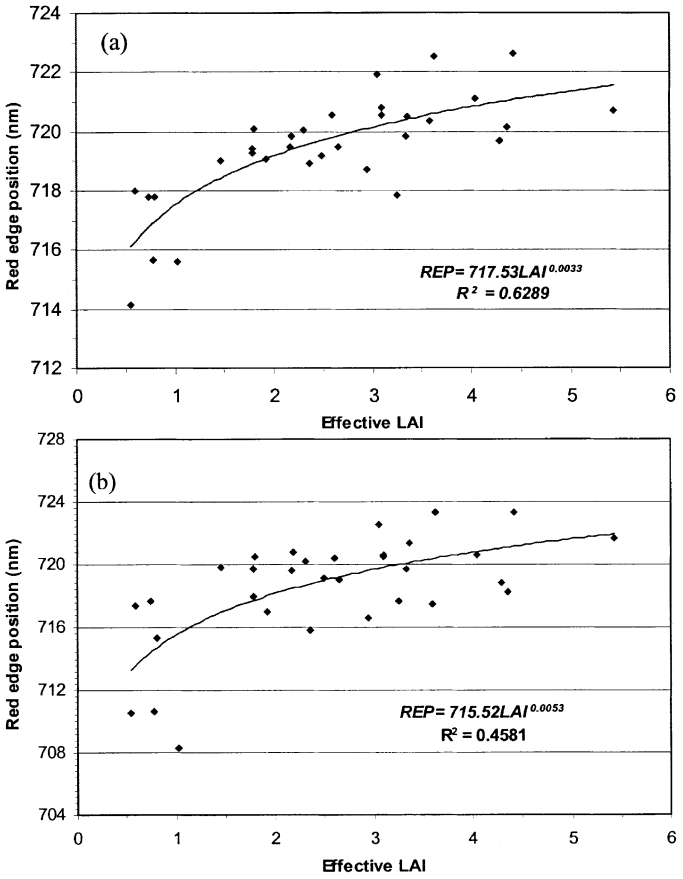

Fig. 3. Forest LAI versus REP extracted with Lagrangian technique. (a) LAI versus REP (polynomial). (b) LAI versus REP (five-point).

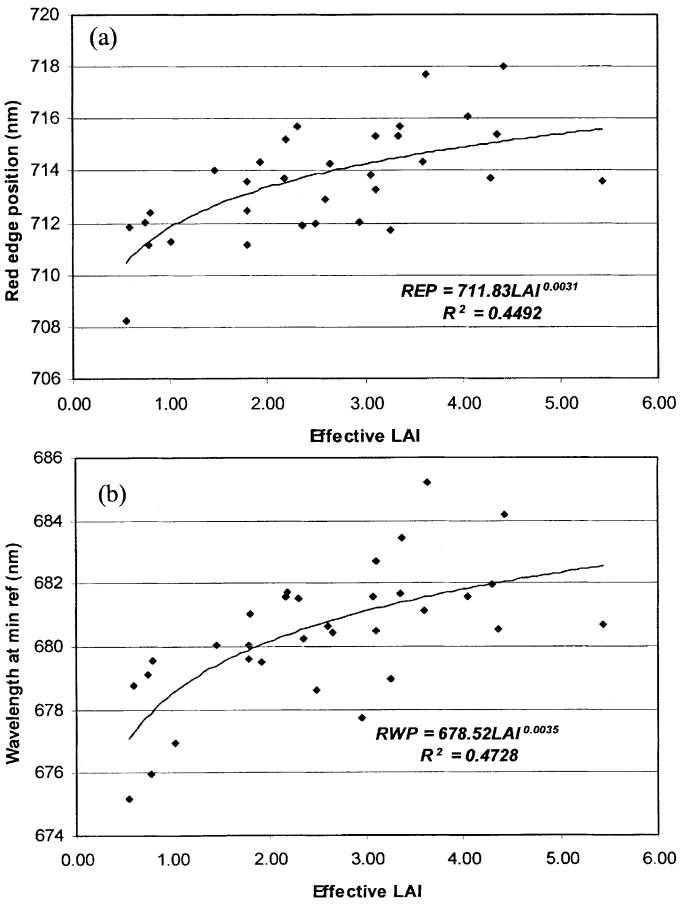

Fig. 4. Forest LAI versus two red edge parameters extracted with the IG modeling approach. (a) LAI versus REP. (b) LAI versus REP (minimum reflectance position).

fitted using a standard numerical procedure, an iterative optimization fitting procedure, and a linearized fitting approach [28] with spectral reflectance data acquired in laboratory or from airborne platforms. In this study, we just used a linearized fitting approach to determine and test the two red edge parameters. Following this approach, mean reflectances are determined for spectral regions 670–685 nm and 780–795 nm to provide estimates of R_0 and R_s. The best estimates of R_0 and R_s can be used with the transformation equation

$$B(\lambda) = \left\{ -\ln \left[\frac{R_s - R(\lambda)}{R_s - R_o} \right] \right\}^{1/2} \tag{9}$$

to yield $B(\lambda)$ as a linear function of λ. Thus a linear regression between B and λ for reflectance data in the spectral range of 685–780 nm yields best fit coefficients a_0 and a_1 that are related to the IG model spectral parameters

$$\lambda_0 = \frac{-a_0}{a_1} \tag{10}$$

$$\sigma = \frac{1}{\sqrt{2}a_1}. \tag{11}$$

In this study, we also used reflectance from 13 Hyperion bands to fit the IG model in order to extract the two red edge parameters for each spectral sample.

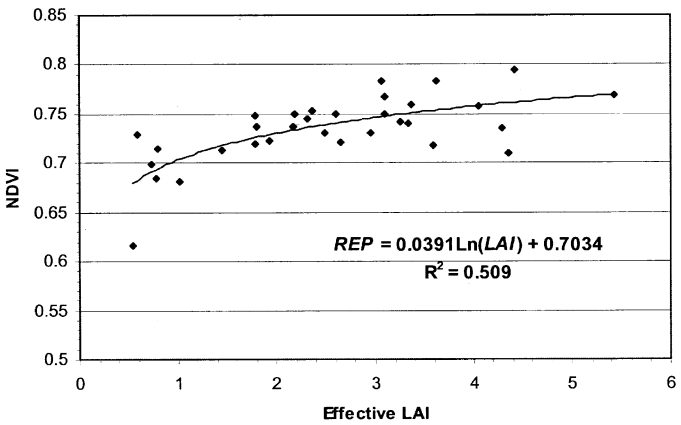

Fig. 5. Forest LAI versus NDVI calculated with NIR band (783.48 nm) and red band (671.62 nm). This NDVI's result is used for comparison with results derived with two red edge parameters REP and RWP.

IV. Results and Analysis

A. Correlation of Two Red Edge Parameters With LAI

Corresponding to each of the LAI measurement sites, one to four homogenous pixel spectra were extracted from the calibrated Hyperion image. The extracted spectra were averaged at each LAI plot for red edge parameter calculation. Using the four different calculation methods, we calculated each red edge parameter for all 32 spectral samples corresponding to the 32

TABLE I
CORRELATION COEFFICIENTS AND VARIATION RANGES OF RED EDGE PARAMETERS, EXTRACTED FROM HYPERION DATA USING FOUR APPROACHES, WITH FOREST LAI ($n = 32$)

Approach	REP		RWP	
	R^2	Range (nm)	R^2	Range (nm)
4-point	0.6457	718.5-724.5	0.6572	683.9-688.4
Polynomial	0.6525	714.1-722.8	0.5668	673.0-682.0
Lagrangian (poly)	0.6289	714.1-722.6	n/a	n/a
(5-p)	0.4581	708.3-723.3	n/a	n/a
IG model	0.4492	708.2-718.1	0.4728	675.2-685.3

Note: R^2(with NDVI) = 0.5090; Lagrangian (poly) is using three 1st derivative bands (713, 720, 727 nm), calculated by the polynomial method; Lagrangian (5-p) is using 5 original Hyperion bands (702.12, 712.29, 722.46, 732.63 and 742.8 nm).

TABLE II
SUMMARY OF THE RELATIVE PERFORMANCES OF THE FOUR APPROACHES

method	Implementation	Required spectral type	Suitability for discont. spectra	REP bias	Correlation with LAI
4-point interpolation	easy	reflectance	yes	longer w.	high
polynomial fitting	moderate	reflectance	no	proper	high
Langragian interpolation	moderate	derivative	no	proper	medium
IG modeling	difficult	reflectance	no	proper	low

Note: discont.--discontinuous, w.--wavelength.

LAI measurements. The correlation results of the red edge parameters with forest LAI are shown in Fig. 1 for the four-point approach, Fig. 2 for the polynomial, Fig. 3 for the Lagrangian interpolation (REP only), and Fig. 4 for the IG modeling. For purposes of comparison, we also present the correlation result produced using a traditional normalized difference vegetation index (NDVI) (Fig. 5), constructed with two Hyperion bands centered at 671.62 and 783.48 nm.

The first two methods generated similar results except the polynomial approach produced a slightly lower R^2 value than the four-point approach with a RWP parameter. The IG modeling method produced the lowest R^2 values. The correlation result of REP generated using the Lagrangian method with the three first-derivative bands calculated from polynomial fitting is slightly lower than those produced using the first two approaches, but it is much poorer if calculated using the five original reflectance bands. Among the varied ranges of the REP and RWP parameters produced with these different approaches, the four-point approach generated a narrower range and slightly higher REP and RWP values (Table I).

B. Performance of the Four Approaches

Among the four approaches, both red edge parameters derived with the four-point approach are good. This method can be easily done, as it only requires four bands. Therefore, it is the most practical. The effectiveness of the four-point interpolation used for extracting REP was also demonstrated by [16] who used a Spectron SE590 with a spectral resolution of 11 nm from a helicopter at an altitude of 300 m and by [13] with AVIRIS data from bands 29 (674.4 nm), 31 (694.0 nm), 36 (743.0 nm), and 40 (782.2 nm) to approximate the red edge reflectance curve. However, they did not test RWP, which produced results similar to those produced by REP. The reflectance curve fitted with the polynomial approach almost approximates the actual spectral properties in the red edge region. Moreover, the high-order polynomial approach can deal with the multimodal reflectance spectrum in its first derivative [12], while the other three cannot. However, its implementation needs more computation time. For the Lagrangian technique, if the first derivative spectra are available, we can simply take three bands containing the maximum first derivative reflectance value to determine REP. However, if the first derivative spectra are not available (as is the case for multispectral remote sensing data), this method cannot be used. The correlation result with the REP directly obtained by calculating the three first-derivative bands from the five original reflectance bands proved this point. The IG modeling method was tested for the first time with satellite-based hyperspectral data ($\sim$10-nm spectral resolution). The poor results generated with this method might be due to the fact that the Hyperion reflectance data were still contaminated by the atmospheric effects even though atmospheric correction had been done. It could also be caused by a less desirable band setting of the Hyperion sensor for the IG model. Table II is a summary of performances of the four approaches. The four-point interpolation is the best, followed by polynomial fitting. The Langragian technique may not have practical value, while the IG model needs further testing.

Fig. 5 presents the result produced using a traditional NDVI with LAI. Compared to the results based on the red edge parameters, the first two approaches and the Lagrangian interpolation with curve-fitted first-derivative spectra can produce better results than those obtained by NDVI. This is because the NDVI is unlikely to provide reliable estimates of LAI in forests due to independent variation of canopy cover which affects the index [11], and due to its saturation at relatively low LAI values [16]. This also conversely proves that the red edge parameters are relatively robust for estimating forest LAI under variation of canopy structure and soil background condition. In this

study, LAI measurements were taken from various forest plots that cover a relatively wide range of actual forest LAI values (0.5–7.0), and the different LAI plots represent varying background (e.g., varying bare soil, grasses, shrub, and understory cover percentages). In addition, the hyperspectral data have been corrected for the atmospheric effects. The experiment results (relations of red edge parameters with LAI) should have a certain level of applicability to other conifer canopy types using Hyperion data. Practically, the REP may be better than the RWP, since the range of RWP is relatively narrower than that of REP, leaving it vulnerable to measuring error.

V. Conclusion

Since only four bands in reflectance are needed, the four-point approach is the most practical for extracting the two red edge parameters from Hyperion data for forest LAI estimation. It may also be suitable for multispectral remote sensing if the band setting is appropriate. Although the polynomial fitting approach also has practical value if hyperspectral data (spectral resolution narrower than 10 nm like Hyperion data) are available, it requires computation time. Moreover, it is not useful for multispectral data. Because the first derivative spectra frequently are not directly available for most multi/hyperspectral sensors, use of the Lagrangian technique is less practical. The IG modeling did not work well with the linear fitting approach tested in this study.

Acknowledgment

The authors acknowledge the assistance in the field work by G. Defossé, F. Farías, and M. C. Frugoni, which is greatly appreciated.

References

[1] J. Chen and J. Cihlar, "Retrieving leaf area index of boreal conifer forests using Landsat TM images," *Remote Sens. Environ.*, vol. 55, pp. 153–162, 1996.

[2] K. S. Fassnacht, S. T. Gower, M. D. MacKenzie, E. V. Nordheim, and T. M. Lillesand, "Estimating the leaf area index of north central Wisconsin forests using the Landsat Thematic Mapper," *Remote Sens. Environ.*, vol. 61, pp. 229–245, 1997.

[3] P. Gong, R. Pu, and J. R. Miller, "Coniferous forest leaf area index estimation along the Oregon transect using compact airborne spectrographic imager data," *Photogramm. Eng. Remote Sens.*, vol. 61, no. 9, pp. 1107–1117, 1995.

[4] J. D. White, S. W. Running, R. Nemani, R. E. Keane, and K. C. Ryan, "Measurement and remote sensing of LAI in Rocky Mountain Montane ecosystems," *Can. J. Forest Res.*, vol. 27, pp. 1714–1727, 1997.

[5] S. W. Running, R. R. Nemani, D. L. Peterson, L. E. Band, D. F. Potts, L. L. Pierce, and M. A. Spanner, "Mapping regional forest evapotranspiration and photosynthesis by coupling satellite data with ecosystem simulation," *Ecology*, vol. 70, no. 4, pp. 1090–1101, 1989.

[6] D. L. Peterson, M. A. Spanner, S. W. Running, and K. B. Teuber, "Relationship of Thematic Mapper simulator data to leaf area index of temperate coniferous forests," *Remote Sens. Environ.*, vol. 22, pp. 323–341, 1987.

[7] P. J. Curran, J. L. Dungan, and H. L. Gholz, "Seasonal LAI of slash pine estimated with Landsat TM," *Remote Sens. Environ.*, vol. 39, pp. 3–13, 1992.

[8] N. J. Smith, G. A. Borstad, D. A. Hill, and R. C. Kerr, "Using high-resolution airborne spectral data to estimate forest leaf area and stand structure," *Can. J. Forest Res.*, vol. 21, pp. 1127–1132, 1991.

[9] M. A. Spanner, L. L. Pierce, D. L. Peterson, and S. W. Running, "Remote sensing of temperate coniferous forest leaf area index: The influence of canopy closure, understory vegetation and background reflectance," *Int. J. Remote Sens.*, vol. 11, pp. 95–111, 1990.

[10] G. Guyot, F. Baret, and S. Jacquemoud, "Imaging spectroscopy for vegetation studies," *Imaging Spectroscopy: Fundamentals and Prospective Application*, pp. 145–165, 1992.

[11] R. R. Nemani, L. L. Pierce, S. W. Running, and L. E. Band, "Forest ecosystem processes at the watershed scale: Sensitivity to remotely-sensed leaf area index estimates," *Int. J. Remote Sens.*, vol. 14, no. 13, pp. 2519–2534, 1993.

[12] N. N. H. Horler, M. Dockray, and J. Barber, "The red edge of plant leaf reflectance," *Int. J. Remote Sens.*, vol. 4, no. 2, pp. 273–288, 1983.

[13] C. E. Leprieur, "Preliminary evaluation of AVIRIS airborne measurements for vegetation," in *Proc. 9th EARSeL Symp.*, Espoo, Finland, June 27–July 1 1989, pp. 1–6.

[14] P. J. Curran, W. R. Windham, and H. L. Gholz, "Exploring the relationship between reflectance red edge and chlorophyll concentration in slash pine leaves," *Tree Physiol.*, vol. 15, pp. 203–206, 1995.

[15] F. Baret, I. Champion, G. Guyot, and A. Podaire, "Monitoring wheat canopies with a high spectral resolution radiometer," *Remote Sens. Environ.*, vol. 22, pp. 367–378, 1987.

[16] F. M. Danson and S. E. Plummer, "Red-edge response to forest leaf area index," *Int. J. Remote Sens.*, vol. 16, no. 1, pp. 183–188, 1995.

[17] M. J. Belanger, J. R. Miller, and M. G. Boyer, "Comparative relationships between some red edge parameters and seasonal leaf chlorophyll concentrations," *Can. J. Remote Sens.*, vol. 21, no. 1, pp. 16–21, 1995.

[18] T. P. Dawson and P. J. Curran, "A new technique for interpolating the reflectance red edge position," *Int. J. Remote Sens.*, vol. 19, pp. 2133–2139, 1998.

[19] R. Munden, P. J. Curran, and J. A. Catt, "The relationship between red edge and chlorophyll concentration in Broadbalk winter wheat experiment at Rothamsted," *Int. J. Remote Sens.*, vol. 15, no. 3, pp. 705–709, 1994.

[20] I. Filella and J. Peñuelas, "The red edge position and shape as indicators of plant chlorophyll content, biomass and hydric status," *Int. J. Remote Sens.*, vol. 15, no. 7, pp. 1459–1470, 1994.

[21] K. O. Niemann, "Remote sensing of forest stand age using airborne spectrometer data," *Photogramm. Eng. Remote Sens.*, vol. 61, no. 9, pp. 1119–1127, 1995.

[22] G. Vane and A. F. H. Goetz, "Terrestrial imaging spectroscopy," *Remote Sens. Environ.*, vol. 24, pp. 1–29, 1988.

[23] J. R. Miller, J. Wu, M. G. Boyer, M. Belanger, and E. W. Hare, "Season patterns in leaf reflectance red edge characteristics," *Int. J. Remote Sens.*, vol. 12, no. 7, pp. 1509–1523, 1991.

[24] S. Ungar, J. Pearlman, J. Mendenhall, and D. Reuter, "Overview of the Earth Observing One (EO-1) mission," *IEEE Trans. Geosci. Remote Sensing*, to be published.

[25] P. Gong, R. Pu, G. Biging, and M. R. Larrieu, "Estimation of forest leaf area index using vegetation indices derived from Hyperion hyperspectral data," *IEEE Trans. Geosci. Remote Sensing*, to be published.

[26] R. Pu, P. Gong, and G. Biging, "Simple calibration of AVIRIS data and LAI mapping of forest plantation in southern Argentina," *Int. J. Remote Sens.*, vol. 24, 2003.

[27] G. F. Bonhan-Carter, "Numerical procedures and computer program for fitting an inverted Gaussian model to vegetation reflectance data," *Comput. Geosci.*, vol. 14, no. 3, pp. 339–356, 1988.

[28] J. R. Miller, E. W. Hare, and J. Wu, "Quantitative characterization of the vegetation red edge reflectance. 1. An inverted-Gaussian reflectance model," *Int. J. Remote Sensing.*, vol. 11, pp. 1775–1795, 1990.

[29] N. K. Patel, C. Patnaik, S. Dutta, A. M. Shekh, and A. J. Dave, "Study of crop growth parameters using airborne imaging spectrometer data," *Int. J. Remote Sens.*, vol. 22, no. 12, pp. 2401–2411, 2001.